Journal of Biomaterials Applications

http://jba.sagepub.com/

Cytotoxicity of Gold Nanoparticles Prepared by Ultrasonic Spray Pyrolysis

R. Rudolf, B. Friedrich, S. Stopic, I. Anzel, S. Tomic and M. Colic

J Biomater Appl published online 6 September 2010
DOI: 10.1177/0885328210377536

The online version of this article can be found at:
http://jba.sagepub.com/content/early/2010/07/22/0885328210377536

Published by:
SAGE
http://www.sagepublications.com

J Biomater Appl OnlineFirst, published on September 6, 2010 as doi:10.1177/0885328210377536

Cytotoxicity of Gold Nanoparticles Prepared by Ultrasonic Spray Pyrolysis

R. RUDOLF,[1,*] B. FRIEDRICH,[2] S. STOPIĆ,[2] I. ANŽEL,[1]
S. TOMIĆ[3] AND M. ČOLIĆ[3,4]

[1]*Faculty of Mechanical Engineering, University of Maribor*
Smetanova 17, SI- 2000 Maribor, Slovenia

[2]*IME Process Metallurgy and Metal Recycling*
RWTH Aachen University, Intzestras 1, 52056 Aachen, Germany

[3]*Institute of Medical Research, Military Medical Academy*
Crnotravska 17, 11002 Belgrade, Serbia

[4]*Medical Faculty, University of Niš, Blvd. Dr Zorana Đinđića 81*
18000 Niš, Serbia

ABSTRACT: The aim of this work was to study the cytotoxicity of different fractions of gold nanoparticles prepared by ultrasonic spray pyrolysis from gold scrap. The target cells were rat thymocytes, as a type of nonproliferating cells, and L929 mouse fibroblasts, as a type of continuous proliferating cells. Fractions 1 and 2, composed of pure gold nanoparticles, as determined by scanning electron microscopy with a combination of energy dispersive X-ray analysis, were nontoxic for thymocytes, but reduced moderately the proliferative activity of L929 cells. The inhibitory effect of fraction 2, containing particles smaller in size than fraction 1, was stronger. Fraction 3, composed of Au and up to 3% Cu was noncytotoxic for thymocytes, but was cytotoxic for L929 cells. Fraction 4, composed of Au and Ag nanoparticles, and fraction 5, composed of Au together with Cu, Ni, Zn, Fe, and In were cytotoxic for both thymocytes and L929 cells. These results suggest that USP enables the synthesis of pure gold nanoparticles with controlled size, even from gold scrap. However, microstructural analyses

*Author to whom correspondence should be addressed.
E-mail: rebeka.rudolf@uni-mb.si

0885-3282/10/00 0001–18 $10.00/0 DOI: 10.1177/0885328210377536

and biocompatibility testing are necessary for their proper selection from more cytotoxic gold nanoparticles, contaminated with other elements of gold alloys.

KEY WORDS: gold nanoparticles, ultrasonic spray pyrolysis, microstructure, cytotoxicity, L929 cells, thymocytes.

INTRODUCTION

Gold nanoparticles are of high interest because of their potential application in electrochemistry and medicine as well as for the production of nanodevices [1,2]. Useful properties of nanoscale materials such as the minute size, similar to cellular components and macromolecules, may facilitate their use in medicine for the detection of biological structures and systems and for manipulation of cellular functions [2–4]. Nanoparticles are currently exploited in imaging [5,6], bio-sensing [7,8], and gene and drug delivery [9–11]. However, depending on their structure and physico-chemical properties, nanomaterials may cause adverse health effects. Due to the chemical stability of Au, gold nanoparticles were expected to be biocompatible, as documented in different publications [12–14]. In contrast, there were some reports showing that endocytosed gold nanoparticles may cause cytotoxic effects. Such results suggest that the use of gold nanoparticles as tracers in biomedical imaging and diagnostic tests or carriers for delivery of drugs or biomolecules may be dangerous for health. On the other hand, the cytotoxic effect of gold nanoparticles could be desirable if such materials are designed for the treatment of malignant tumors or the suppression of inflammation and immune response in chronic inflammatory diseases [15,16].

We used a new technology to produce gold nanoparticles from gold scrap by ultrasonic spray pyrolysis (USP). This method enables synthesis of gold nanoparticles of various sizes and shapes, including nanoparticles contaminated with metals from gold alloys. Therefore, the aim of this work was to characterize the different fractions of gold nanoparticles using scanning electron microscopy (SEM) with a combination of energy dispersive X-ray (EDX) analysis and to examine their cytotoxicity *in vitro*.

MATERIALS AND METHODS

Preparation of Gold Nanoparticles from Gold Scraps

A chemically dissolved gold scrap (wt: 58.5% Au; 8.11% Ni; 24.35% Cu; 8.37% Zn; 0.67% rest) from Zlatarna Celje, Slovenia, was used as

a precursor for the synthesis of gold nanoparticles by USP, using an ultrasonic atomizer (Gapusol 9001, RBI/France), containing a reactor with three separated heating zones and an electrostatic precipitator. The synthesis was performed at the IME process metallurgy and Metal Recycling of the RWTH Aachen University in Germany. A similar procedure for production of metal and gold nanoparticles was published previously [17,18]. Briefly, the gold scrap obtained was first dissolved in a water solution of chloric and nitric acid in order to prepare the solution for an aerosol production. The solution was kept overnight and after that passed over to the ultrasonic atomizer. The temperature and pressure control were adjusted using a thermostat and a vacuum pump.

The aerosol produced, resulting from a frequency of 2.5 MHz, was transported by nitrogen/hydrogen gas into a hot reactor, where the aerosol droplets underwent drying, droplet shrinkage, solute precipitation, thermolysis, and sintering to form nanoparticles. Thermal decomposition of the resulting solution was performed at 300°C and 800°C. The nanoparticles were collected in a reaction tube and in a bottle with water and alcohol.

Micro-Structural and Elemental Characterization of Gold Nanoparticles

A scanning electron microscope, Quanta 200 3D equipped with a focused ion beam (FIB) and Pt-gas deposition system, was used for the characterization of the obtained nanopowders. The EDX microanalysis system (EDS) – INCA 350 System was used for quantitative chemical analysis. SEM images were used to observe the surface morphology of particles formed at different parameter sets.

Cytotoxicity Testing

The cytotoxicity of gold nanoparticle fractions was tested using a standard method for measurement of mitochondrial succinic dehydrogenase (SDH) activity in rat thymocytes and L929 mouse fibroblasts. Thymocytes were isolated from the thymuses of Albino Oxford (AO) rats, male, 10 weeks old, bred at the Institute of Medical Research, MMA, Belgrade, Serbia as we previously described [19]. The use of animals for the experiments was in accordance with the Guideline for the Use of Experimental Animals, approved by the Ethical Committee of the Military Medical Academy, Belgrade, Serbia (282-12/2002), which strictly follows the rules of the European Community Guidelines (EEC Directive of 1986; 86/609/EEC). Single cell suspensions of thymocytes

were prepared by teasing the thymuses in an RPMI medium through a steel-mesh. After washing, the thymocytes were counted and then used for cell cultures.

L929 cells, a continuous proliferating mouse fibroblast line (5×10^4/mL), or thymocytes (5×10^6/mL) were cultivated with different gold nanoparticle fractions in flat-bottom 96-well plates (ICN, Costa Mesa, CA; 200 μL/well) in an incubator with CO_2 at 37°C, using complete RPMI medium for 24 h or 3 days. We used different number of cells because their size was significantly different. In addition, our previous results [20] showed that such number of cells formed confluent monolayers in culture. The complete RPMI medium consisted of basic RPMI 1640 medium (Sigma, Munich, Germany), 10% heat inactivated fetal calf serum (FCS) (Sigma), 2 mM L-glutamine (Sigma), and antibiotics (Galenika, Zemun, Serbia) including gentamycin (10 μg/mL), penicillin (100 units/mL), and streptomycin (125 μg/mL). Before the experiment, gold nanoparticle fractions were sonicificated using an ultrasonic bath for 1 h. The working concentrations of the fractions were 25 and 100 μg/mL. The controls were cell cultures without gold nanoparticles.

The first cytotoxic test was based on the determination of succinate dehydrogenase activity (SDA) in thymocytes and L929 cells. After incubation of the cells for the indicated period of time, the medium was carefully removed and the wells were filled with 100 μL of 3-[4,5-dimethylthiazol-2-yl]-2,5 diphenyl tetrazolium bromide (MTT) (Sigma, Munich, Germany) (1 mg/mL), dissolved in the complete RPMI medium. Wells with gold nanoparticle fractions without cells filled with 100 μL of MTT served as controls. In addition, wells with 100 μL of MTT solution served as blank controls. After a 3 h incubation period (37°C, 5% CO_2), 100 μL/well of 10% sodium dodecyl sulphate (SDS) −0.1 N HCL (Serva, Heidelberg, Germany) was added to solubilize intracellularly stored formazan. The plates were incubated overnight at room temperature. The optical density (OD) of the color was then measured at 570 nm in a spectrophotometer (Behring ELISA Processor II, Heidelberg, Germany). The results were expressed as the percentage of OD (as a measure of metabolic activity) compared to the control (cultures without gold nanoparticle fractions), used as follows:

Metabolic activity (%) = (OD of cells cultivated with gold nanoparticles-OD of gold nanoparticles cultivated without cells)/(OD of cells cultivated alone-OD of gold nanoparticles cultivated alone) × 100.

Apoptosis was detected by using propidium iodide (PI) (Sigma) and flow cytometry as we described previously [19]. The method is based on the detection of DNA fragmentation as revealed by the quantification of hypodiploid nuclei. For this purpose, thymocytes (2×10^5) were collected

from the wells by pipeting, then washed with PBS and incubated with 500 μL of PI (10 μg/mL) dissolved in a hypotonic solution (0.1% sodium citrate + 0.1% Triton-X solution in distilled water). Cells were cultivated with PI for 4 h at room temperature and then analyzed by flow cytometry. L929 cells were detached from the plastic surface by using 0.25% trypsine (Serva, Heidelberg, Germany) before staining with PI, as described for thymocytes.

Cell death was determined by staining the thymocytes and L929 cells from cultures with 1% Trypan Blue. The positive cells, identified by light microscopy, were considered as dead, predominantly necrotic cells. The percentages of dead cells were determined on the basis of at least 500 total cells from one well. The percentage of viable cells was calculated as 100% of total cells-% of dead cells. All results were expressed as a mean of triplicates. Additionally, necrosis was confirmed as we previously described [21] using a staining protocol with PI without cell permeabilization and flow cytometry.

Proliferation Assay

L929 cells were cultivated alone or with different fractions of gold nanoparticles for 48 h as described. During the last 18 h of incubation, the cells were pulsed with 1 μCi/well [3H] thymidine (6.7 Ci/mmol, Amersham, Bucks, UK). At the end of incubation time the cultures were treated with 0.25% trypsine (Serva, Heidelberg, Germany) in order to detach the cells from the plastic surface. After harvesting, the radioactivity was counted using a scintillation counter (Beckman). The results were expressed as mean counts per minute (cpm) of triplicates. Proliferation activity was presented in percentages calculated on the basis of the proliferation activity of control cultures.

RESULTS

Microstructural Analysis of Gold Nanoparticles

By using USP, five fractions of gold nanoparticles were produced from the gold scrap. The results of microstructural analysis of the fractions (SEM + EDX) are presented in Table 1 and Figures 1–5. The fraction 1 contained pure gold nanoparticles (120.1 ± 51.0 nm; $n = 29$ measurements) (Table 1, Figure 1), produced at 300°C in a hydrogen atmosphere. This fraction, which was partially agglomerated, was recovered from the reaction tube wall. The fraction 2 (Table 1, Figure 2), produced and recovered similarly, contained partially agglomerated pure

Table 1. Metal content analysis of the fractions of gold nanoparticles.

Elements	Fr. 1 (W%/A%)	Fr. 2 (W%/A%)	Fr. 3 (W%/A%)	Fr. 4 (W%/A%)	Fr. 5 (W%/A%)
Au	100.0/100.0	100.0/100.0	99.1/97.3	61.6/59.4	57.8/28.7
Cu			0.9/2.7		19.2/28.1
Ag				35.4/31.5	
Ni					14.5/24.3
Zn					1.9/2.7
Fe					0.2/0.6
Na				0.2/1.2	
In					0.2/0.2
Cl				2.7/7.8	2.9/4.1
O					1.5/5.3
C					1.7/5.9

Values are given as the mean of 20 different measurements.
W = Weight; A = Atomic.

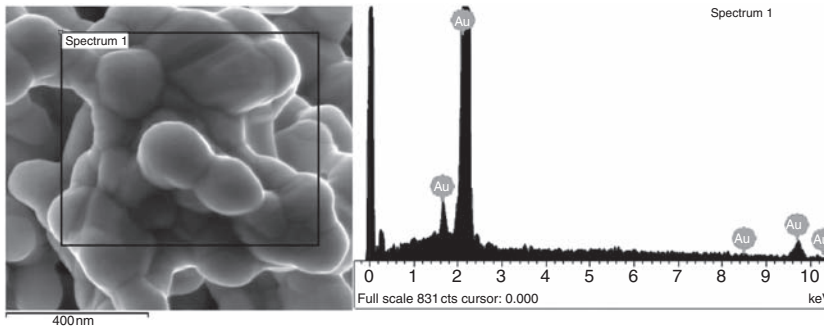

Figure 1. Fraction 1 of gold nanoparticles: SEM image and EDX analysis of elemental content within a representative spectrum.

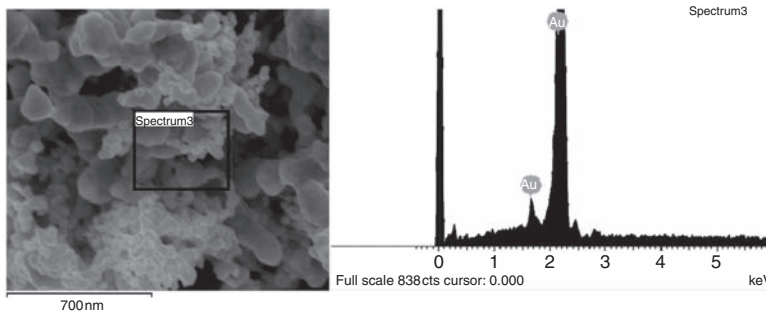

Figure 2. Fraction 2 of gold nanoparticles: SEM image and EDX analysis of elemental content within a representative spectrum.

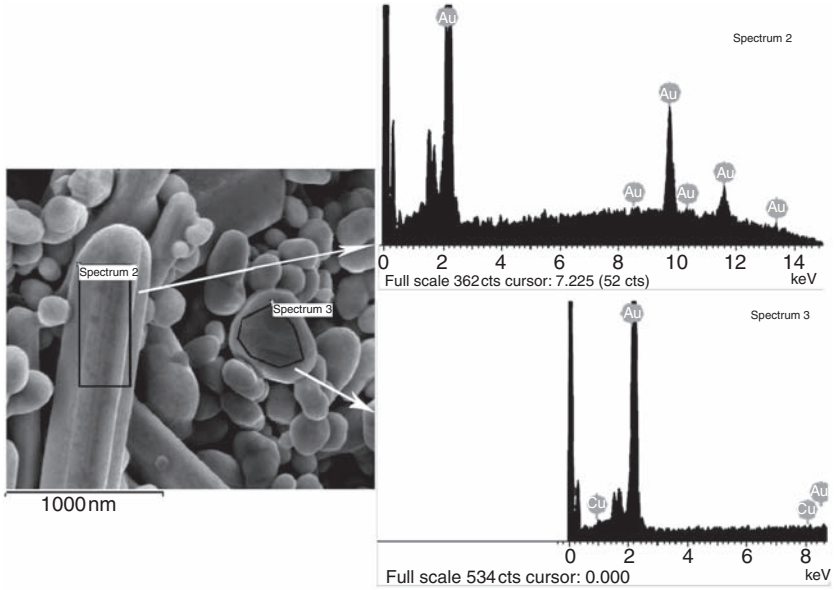

Figure 3. Fraction 3 of gold nanoparticles: SEM image and EDX analyses of elemental content within two marked spectra.

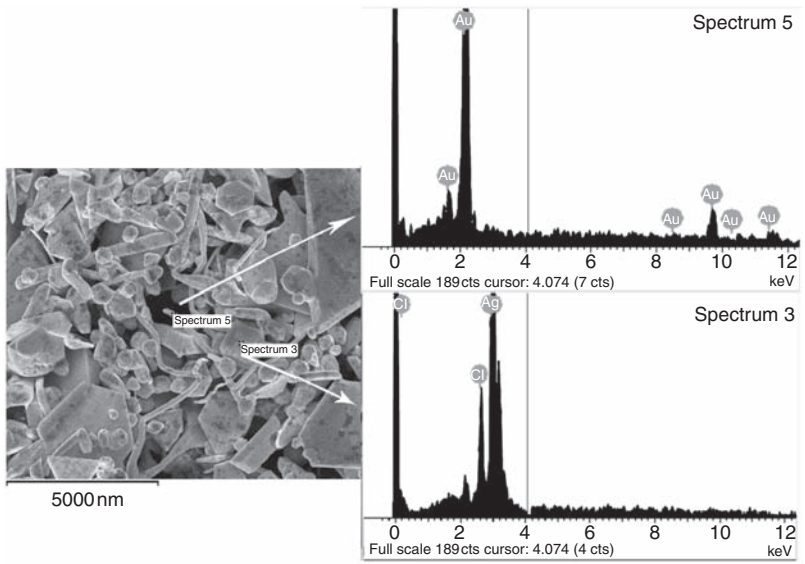

Figure 4. Fraction 4 of gold nanoparticles: SEM image and EDX analyses of elemental content within two marked spectra.

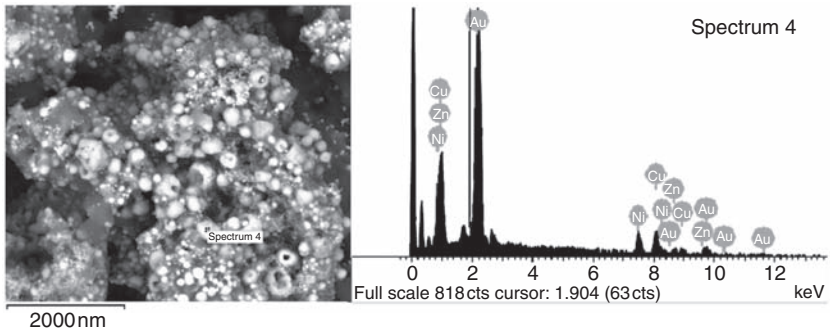

Figure 5. Fraction 5 of gold nanoparticles: SEM image and EDX analysis of elemental content within a representative spectrum.

gold nanoparticles, different in size, mostly spherical, which were smaller than fraction 1 (97.3 ± 49.8 nm; $n = 135$ measurements). Fraction 3, produced at 800°C in a hydrogen atmosphere, contained pure gold nanorods (length $= 3570 \pm 1960$ nm; $n = 25$; width $= 700.5 \pm 200.3$; $n = 25$), spherical-shaped pure gold nanoparticles (362.0 ± 169.0 nm; $n = 98$) and some spherical gold nanoparticles alloyed with Cu (Table 1, Figure 3). Fraction 4 was composed of gold particles micron in size, irregularly shaped, contaminated with AgCl powder. This fraction precipitated before thermal decomposition/atomization took place (Table 1, Figure 4). Fraction 5 (size of particles 253.0 ± 178.3 nm; $n = 100$), recovered from the bottle with water and alcohol, contained gold and alloying elements (Cu, Zn, Ni, Fe, In), as well as contaminations such as Cl, O, and C, originating from nitric and chloride acids (Table 1, Figure 5).

Effect of Gold Nanoparticles on Cellular Metabolic Functions

The cytotoxicity of gold nanoparticle fractions was tested using rat thymocytes as a type of non-proliferating cells and a mouse fibroblast cell line, L929 clone, as a type of proliferating cells. The first screening, MTT test, showed that fractions 1, 2, and 3, at both concentrations (25 and 100 μg/mL) were noncytotoxic for thymocytes. A higher concentration of fractions 1 and 2, and lower concentration of fraction 3 reduced moderately the metabolic activity of L929 cells, especially after prolonged cultivation (3 days). The inhibitory effect of fraction 2 on the metabolic activity of L929 cells was stronger than fraction 1. A higher concentration of fraction 3 reduced the metabolic activity of the cells by about 80% (day 3), compared to the control. Fractions 4 and

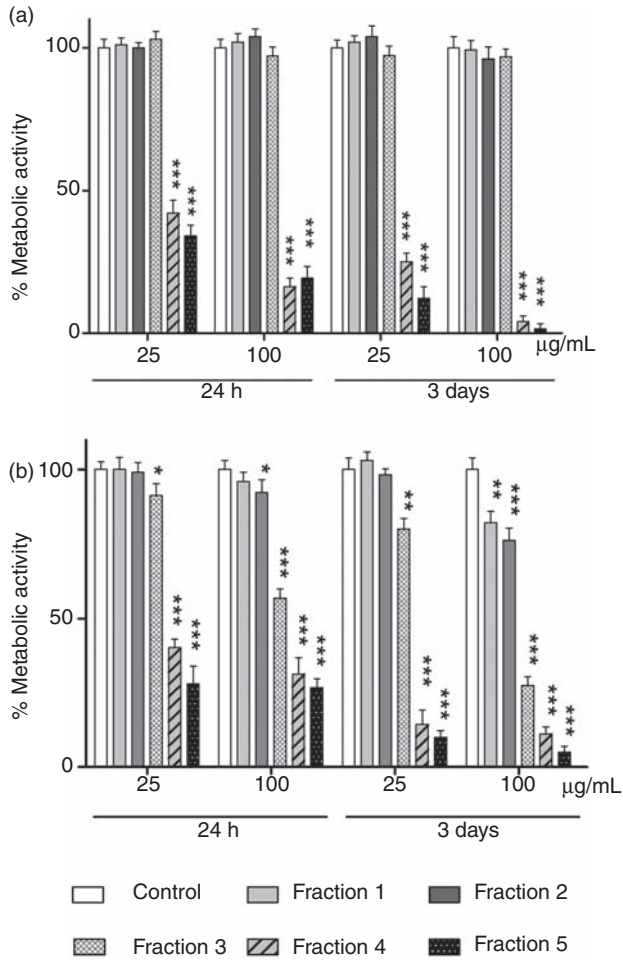

Figure 6. Effect of different fractions of gold nanoparticles on the metabolic activity of: (a) thymocytes and (b) L929 cells. $^{*}p < 0.05$; $^{**}p < 0.01$; $^{***}p < 0.005$ compared to corresponding control.

5 reduced significantly the metabolic activity of both thymocytes and L929 cells, and their effect was dose- and time-dependent (Figure 6).

Mechanisms of Cytotoxicity of Gold Nanoparticles

To study whether inhibition of the metabolic activity of L929 cells is due to the cytotoxic or anti-proliferative effect of gold nanoparticles,

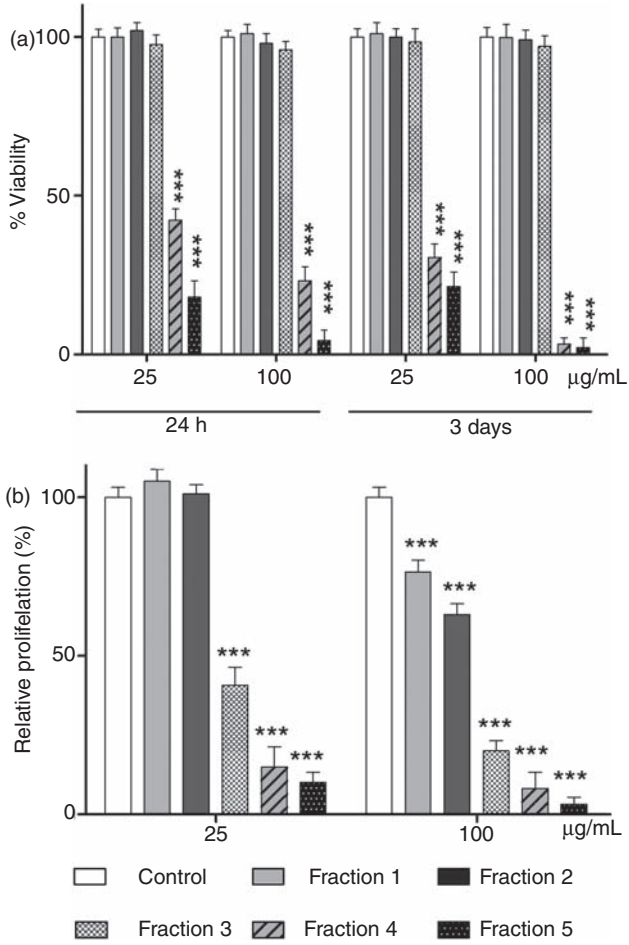

Figure 7. Effect of different fractions of gold nanoparticles on the (a) viability and (b) relative proliferation of L929 cells. $^{***}p < 0.005$ compared to corresponding control.

the viability and proliferative assays were performed. The results (Figure 7(a)) show that neither concentration of fractions 1, 2 and 3 was cytotoxic for L929 cells, as judged by the preserved viability of the cells. However, both concentrations of fractions 4 and 5 were cytotoxic, since cell viability was significantly decreased (25 µg/mL) or almost completely reduced (100 µg/mL).

When proliferation was studied (Figure 7(b)), it could be seen that higher concentrations of all fractions suppressed cell growth, insofar as fraction 1 showed the lowest and fraction 5 the highest inhibitory effect.

Table 2. Effect of different fractions of gold nanoparticles on apoptosis and necrosis of rat thymocytes and L929 cells.

	Thymocytes		L929 cells	
	Apoptosis (%)	Necrosis (%)	Apoptosis (%)	Necrosis (%)
Control	35.1 ± 3.2	5.0 ± 1.6	1.1 ± 0.1	3.6 ± 1.0
Fraction 1 (25 μg/mL)	33.9 ± 3.0	4.5 ± 1.6	0.8 ± 0.1	4.1 ± 1.0
(100 μg/mL)	34.5 ± 2.9	5.0 ± 1.4	1.2 ± 0.0	2.8 ± 0.1
Fraction 2 (25 μg/mL)	37.2 ± 2.8	5.2 ± 1.7	1.0 ± 0.0	3.8 ± 1.2
(100 μg/mL)	36.9 ± 3.0	5.7 ± 1.3	0.9 ± 0.1	5.5 ± 0.8
Fraction 3 (25 μg/mL)	40.0 ± 2.8	6.3 ± 1.5	1.4 ± 0.1	4.8 ± 1.2
(100 μg/mL)	43.5 ± 4.5	6.2 ± 0.7	1.3 ± 0.2	3.8 ± 2.2
Fraction 4 (25 μg/mL)	70.2 ± 3.6***	13.1 ± 2.9**	18.2 ± 1.4***	56.2 ± 4.0***
(100 μg/mL)	59.9 ± 3.0***	16.3 ± 2.5***	2.0 ± 0.0	96.2 ± 0.1***
Fraction 5 (25 μg/mL)	61.2 ± 2.4***	20.2 ± 2.7***	0.5 ± 0.0	96.8 ± 0.2***
(100 μg/mL)	45.7 ± 4.2**	46.1 ± 2.5***	0.2 ± 0.0	100.0 ± 0.0***

The cells were incubated with different concentration of gold nanoparticle fractions. Controls were cell cultures without gold nanoparticles. After 24 h (thymocytes) or 3 days (L929 cells), the cells were stained with propidium iodide as described in Materials and Methods to detect necrosis or apoptosis. Values are given as mean ± standard deviation of sixplicates (thymocytes) or triplicates (L929 cells).
**$p < 0.01$; ***$p < 0.005$, compared to corresponding controls.

Lower concentrations of fractions 1 and 2 were non-inhibitory, whereas both higher and lower doses of fractions 3, 4, and 5 showed strong anti-proliferative activity. Finally, we examined whether the cytotoxic effect of gold nanoparticle fractions on thymocytes and L929 cells was due to apoptosis or necrosis. As shown in Table 2 and Figure 8, spontaneous apoptosis of thymocytes in control cultures was relatively high, whereas the percentage of necrotic cells was low. Fractions 1, 2, and 3 induced neither necrosis nor apoptosis of thymocytes. Fraction 4 caused primarily apoptosis, whereas fraction 5 (especially higher dose) induced primarily necrosis. Both apoptosis and necrosis in control L929 cultures were very low and were not significantly modulated by fractions 1, 2, and 3 of gold nanoparticles. Lower concentration of fraction 4 induced apoptosis and necrosis. Higher concentration of fraction 4 and both concentrations of fraction 5 triggered necrosis of almost all L929 cells.

DISCUSSION

In this article, we showed that USP is an innovative and appropriate technology for the synthesis of pure gold nanoparticles, even from the gold scrap. Additionally, some fractions of gold particles, contaminated with alloying elements were produced. Therefore, apart from SEM, EDX analysis of the nanoparticles is necessary for the explanation of biocompatibility tests.

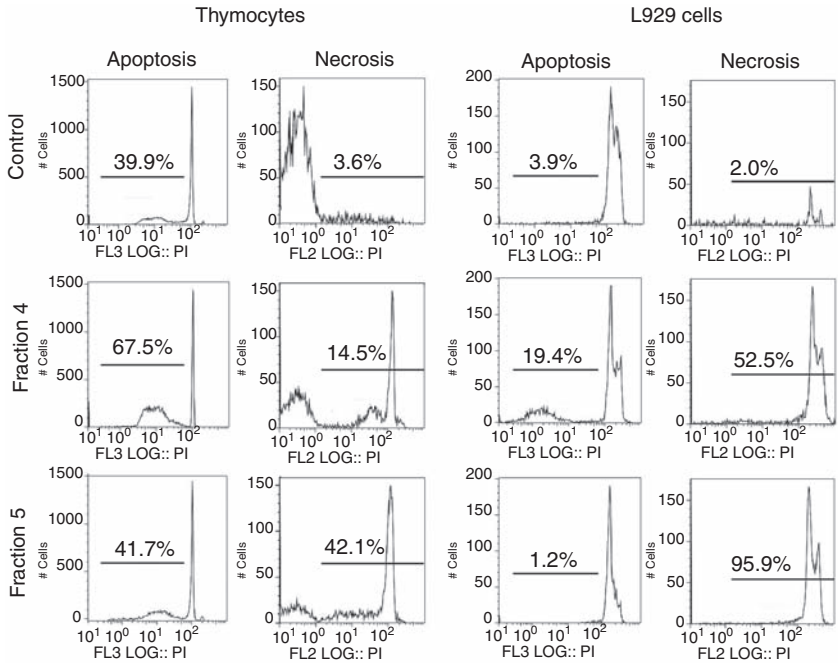

Figure 8. Effect of fractions 4 and 5 of gold nanoparticles on the apoptosis and necrosis of rat thymocytes and L929 cells. The cells were incubated with the fraction 4 (25 μg/mL) or fraction 5 (100 μg/mL) for 24 h (thymocytes) or 3 days (L929 cells). The control cells were cultivated likewise but without gold nanoparticles. The cells were stained with propidium iodide as described in Materials and Methods to detect necrosis or apoptosis and analyzed by flow cytometry.

We used two types of target cells for biocompatibility assays: L929 fibroblasts and rat thymocytes. L929 cells are recommended by ISO standards [22] as a first screening tool for biocompatibility studies of biomaterials. In our previous papers [19,20] we demonstrated that rodent thymocytes are an even more sensitive target for testing the cytotoxicity of different alloys and metal ions released from the alloys in culture medium during conditioning.

Pure gold nanoparticles (fractions 1 and 2), mostly spherical in size, were produced by USP in a hydrogen atmosphere, by decreasing the temperature from 800°C to 300°C. We showed that neither of these fractions of gold nanoparticles was directly cytotoxic for rat thymocytes, but at higher concentrations (100 μg/mL) a reduction of the proliferative activity of L929 cells was observed. The absence of a toxic effect of pure gold nanoparticles on thymocytes may be explained by the fact that

these cells did not ingest gold nanoparticles and that Au was not released from the particles in the culture medium [19].

In contrast, L929 cells are phagocytic [23] and the inhibitory effect of particles on the metabolic activity of these cells, seen after prolonged cultivation (3 days) and which is most probably associated with lower number of cells in culture due to reduced proliferation, could be a consequence of the interference of ingested particles with the signaling mechanisms involved in cellular proliferation. Such a hypothesis is based on other studies, which demonstrated that ingested nanoparticles by fibroblasts in culture, although noncytotoxic, reduced cellular proliferation by inducing a transient oxidative stress [24], or affecting cytoskeleton architecture [25]. It is also possible that proliferation processes may be influenced by disturbing cell-cell contracts by gold nanoparticles attached to the surface of L929 cells.

Up to now, gold nanoparticles were described as nontoxic both *in vitro* and *in vivo* [12,26] due to the chemical stability of Au. However, some studies suggested that gold nanoparticles, especially those prepared by chemical modification to improve their water solubility, are toxic to different cells. Pan et al. [3] have shown that water-soluble gold nanoparticles, stabilized by triphenylphosphine derivatives, showed size-dependent cytotoxicity on epithelial cells, connective tissue fibroblasts, macrophages, and melanoma cells. Gold particles, 1.4 nm in size, were more toxic then larger size particles. In contrast, smaller gold compounds such as Tauredon, a drug used for the treatment of chronic inflammatory diseases [16,27,28], and gold nanoparticles larger than 15 nm were noncytotoxic. These authors also provided evidence that chemicals used for surface modification of gold nanoparticles did not induce the cytotoxic effect. The cytotoxicity of gold nanoparticles may also depend on their uptake. It has been shown that smaller particles are generally taken up better, reaching a maximum of about 40–50 nm. Smaller particles also have a higher surface over volume ratio, leading to a greater reactive surface when the same mass of gold is internalized [29,30]. Therefore, the higher inhibitory effect of fraction 2, (which contained gold nanoparticles lower in size than fraction 1) on the proliferation of L929 cells obtained in our study, is in line with these results. It is interesting that the mode of cell death also depended on the size of particles, in that 1.4 nm particles caused predominantly necrosis, whereas closely related particles 1.2 nm in diameter induced predominantly apoptosis [3].

Generally, the lower toxicity of gold nanoparticles in our culture model could be explained by the lower capability of L929 cells, which are not professional phagocytes, to internalize the particles. In addition, our

pure gold nanoparticle fractions were partially agglomerated and the ultrasonic treatment before their use in culture experiments was not sufficient to disperse them completely. Furthermore, a reaggregation process which occurred in the culture medium, leading to formation of some micron-sized particles, might have decreased phagocytosis. Therefore, in future experiments it is necessary to optimize the dispersibility of particles in order to understand better the mechanisms of their phagocytosis and biological effects.

The much higher toxicity of gold nanoparticles, which contained contaminated metals, could be explained by the toxic effect of not only ingested nanoparticles, but also metal ions released from the particles, either in the culture medium or intracellularly following phagocytosis. It seems that the cytotoxicity of these particles (fractions 3, 4, and 5) depends on the composition of the particles and the type of contaminating micro-alloying elements and their quantity.

Fraction 3 contained nanorods and spherical nanoparticles, much less aggregated then fractions 1 and 2. This difference was probably due to the different temperature used for decomposition/atomization of the gold scrap solution, 800°C (fraction 3 vs. 300°C, fractions 1 and 2). In this context, the use of gold nanorods in biomedicine could be beneficial [31]. Tréguer-Delapierre et al. [32], reported that gold nanorods possess two different resonance modes, in contrast to the single one developed for spherically symmetric gold particles, which is independent of size. These two, separate modes, are due to electron oscillation across and along the longitudinal axis of the nanorods and are termed the transverse and longitudinal modes, respectively. The latter is extremely sensitive to the aspect ratio of the rod (resonance shifts by approximately 100 nm for a change in aspect ratio of 1 unit) [32]. The significant inhibitory effect of fraction 3, which contained not only pure gold nanoparticles, but also some particles contaminated with a small amount of Cu (up to 3%), on L929 cells, could be a consequence of the additional influence of Cu^{2+} ions released intracellularly. The absence of cytotoxic effect of fraction 3 on thymocytes could be explained by the fact that the concentration of Cu^{2+} ions released in the culture medium was not sufficient to trigger cytotoxicity of nonphagocytic cells. It has been shown that Cu ions are toxic to L929 cells and gingival fibroblasts at relatively high concentrations (0.33–1 mmol L^{-1}) [33]. Our previous results showed that concentrations of Cu lower than 8.0 ppm were not cytotoxic [20]. It is known that the quantity of released Cu ions from a Cu-based alloy does not depend on its relative mass concentration but rather on corrosion behavior of Cu in the alloy. Therefore, to make clearer conclusion about possible Cu toxicity in our culture model it is necessary to know the

kinetics of Cu release after ingestion of the particles and its intracellular concentration. Additionally, the higher cytotoxicity of fraction 3 could be due to the higher phagocytosis of particles by L929 cells compared to the gold nanoparticles of fractions 1 and 2. If the anti-proliferative effect of fraction 3 is influenced by phagocytozed particles, it is likely that this does not come from the rod-shaped gold particles, but rather from the spherical ones, because rod-shaped particles are taken up very poorly in general due to greater membrane wrapping time required to enclose elongated particles [34]. Therefore, much more sensitive techniques should be additionally applied to measure intracellular uptake of nanogold particles of different shape and size.

The manifested toxicity of fraction 4 and fraction 5, both on thymocytes and L929 cells, is most probably a result of the predominant effect of contaminating microelements which may act synergistically. Fraction 4 contained Au and Ag. Since this fraction is micron in size, one can postulate that Ag, released from the particles, is the dominant toxic compound. Numerous studies confirmed that Ag could be released from dental alloys and that Ag ions exert cytotoxicity [35,36]. The most toxic effect of fraction 5 could be explained by the synergistic effect of different elements such as Ni, Zn, and Cu. This fraction was formed in a bottle with water/alcohol, most probably as a consequence of the different composition temperature of chloride–nitrate mixture containing gold and microalloying elements. All these elements are toxic and their effect depends on the type of cells and concentrations of released ions from alloys as well as the duration of their exposure to cells in culture [37–39]. We demonstrated that the lower concentration of fraction 5 (25 μg/mL) induced both apoptosis and necrosis, whereas higher concentrations (100 μg/mL) caused predominantly necrosis. A relatively high spontaneous apoptosis of thymocytes in culture is in line with previous numerous publications (reviewed in [40]), as a result of death by neglect of non-positively selected thymocytes *in vivo*. Apoptosis and necrosis are considered functionally and morphologically distinct forms of cell death. However, the observation that cells triggered to undergo apoptosis will die by necrosis when the intracellular energy level is low (depletion of ATP) has altered this concept [41]. Based on these results, it can be postulated that high concentrations of Cu, Ni, and Zn released in the culture medium from this fraction blocked mitochondrial or glycolytic ATP generation and caused necrosis. In this context our results showed higher susceptibility of L929 cells to necrosis, compared to thymocytes. When the levels of these ions were lower, the threshold ATP concentration was sufficient to execute the apoptotic program [41].

CONCLUSION

In conclusion, our results suggest that USP enables the synthesis of pure gold nanoparticles with controlled sizes from gold scrap. However, further microstructural analysis and biocompatibility studies are necessary for their proper selection from more toxic gold nanoparticles, which are contaminated with other microelements. In addition, a detailed thermodynamic analysis is required in order to estimate the processes of thermal decomposition, depending on the gold scrap composition, and thus better separation and dispersion of pure gold nanoparticles.

ACKNOWLEDGMENTS

This article is part of EUREKA Programme E!4953 GoNano and Military Medical Academy, Belgrade project VMA/07-10/B.18.

REFERENCES

1. Xiong, X. and Busnaina, A. Direct Assembly of Nanoparticles for Large-scale Fabrication of Nanodevices and Structures, *J. Nanopart. Res*., 2008: **10**: 947–954.
2. Chithrani, B.D., Ghazani, A.A. and Chan, W.C. Determining the Size and Shape Dependence of Gold Nanoparticle Uptake into Mammalian Cells, *Nano Lett*., 2006: **6**: 662–668.
3. Pan, Y., Neuss, S., Leifert, A. et al. Size-dependent Cytotoxicity of Gold Nanoparticles, *Small* 2007: **3**: 1941–1949.
4. Huang, X., El-Sayed, I.H., Yi, X. and El-Sayed, M.A. Gold Nanoparticles: Catalyst for the Oxidation of NADH to NAD(+), *J. Photoch. Photobio. B*., 2005: **81**: 76–83.
5. Chan, L.Y., Sung, J.J., Chan, F.K., To, K.G., Lau, J.Y. and Chung, S.C. Tissue Injury of Injection Gold Probe, *Gastrointest. Endosc*., 1998: **48**: 291–295.
6. Bruchez Jr, M., Moronne, M., Gin, P., Weiss, S. and Alivisatos, A.P. Semiconductor Nanocrystals as Fluorescent Biological Labels, *Science*, 1998: **281**: 2013–2016.
7. Karhanek, M., Kemp, J.T., Pourmand, N., Davis, R.W. and Webb, C.D. Single DNA Molecule Detection Using Nanopipettes and Nanoparticles, *Nano Lett*., 2005: **5**: 403–407.
8. Taton, T.A., Lu, G. and Mirkin, C.A. Two-Color Labeling of Oligonucleotide Arrays via Size-selective Scattering of Nanoparticle Probes, *J. Am. Chem. Soc*., 2001: **123**: 5164–5165.
9. Panyam, J. and Labhasetwar, V. Biodegradable Nanoparticles for Drug and Gene Delivery to Cells and Tissue, *Adv. Drug Deliv. Rev*., 2003: **55**: 329–347.

10. Yang, P.H., Sun, X., Chiu, J.F., Sun, H. and He, Q.Y. Transferrin-mediated Gold Nanoparticle Cellular Uptake, *Bioconjugate Chem*., 2005: **16**: 494–496.
11. Kohler, N., Sun, C., Wang, J. and Zhang, M. Methotrexate-modified Superparamagnetic Nanoparticles and their Intracellular Uptake into Human Cancer Cells, *Langmuir*, 2005: **21**: 8858–8864.
12. Connor, E.E., Mwamuka, J., Gole, A., Murphy, C.J. and Wyatt, M.D. Gold Nanoparticles are Taken up by Human Cells but do not Cause Acute Cytotoxicity, *Small*, 2005: **1**: 325–327.
13. Tkachenko, A.G., Xie, H., Liu, Y. et al. Cellular Trajectories of Peptide-modified Gold Particle Complexes: Comparison of Nuclear Localization Signals and Peptide Transduction Domains, *Bioconjugate Chem.*, 2004: **15**: 482–490.
14. Shukla, R., Bansal, V., Chaudhary, M., Basu, A., Bhonde, R.R. and Sastry, M. Biocompatibility of Gold Nanoparticles and Their Endocytotic Fate Inside the Cellular Compartment: A Microscopic Overview, *Langmuir*, 2005: **21**: 10644–10654.
15. Tsoli, M., Kuhn, H., Brandau, W., Esche, H. and Schmid, G. Cellular Uptake and Toxicity of Au55 Clusters, *Small*, 2005: **1**: 841–844.
16. DeWall, S.L., Painter, C., Stone, J.D. et al. Noble Metals Strip Peptides from Class II MHC Proteins, *Nat. Chem. Biol.*, 2006: **2**: 197–201.
17. Stopic, S., Friedrich, B., Raic, K., Vulkov-Husovic, T. and Dimitrijevic, M. Characterisation of Nano-Powder Morphology Obtained by Ultrasonic Spray Pyrolysis, *Metalurgija*, 2008: **14**: 41–54.
18. Stopic, S., Friedrich, B., Rudolf, R. and Anžel, I. (2009). Gold Nanoparticles Produced by Ultrasonic Spray Pyrolysis, In: *Proceedings of the 5th International Conference on Gold Science Technology and its Applications*, Heidelberg, 26–29 July, p. 385.
19. Colic, M., Stamenkovic, D., Anzel, I., Lojen, G. and Rudolf, R. The Influence of the Microstructure of High Noble Gold-Platinum Dental Alloys on their Corrosion and Biocompatibility *In vitro*, *Gold Bull*., 2009: **42**: 34–47.
20. Colic, M., Rudolf, R., Stamenkovic, D. et al. Relationship Between Microstructure, Cytotoxicity and Corrosion Properties of a Cu-Al-Ni Shape Memory Alloy, *Acta Biomater.*, 2009: **6**: 308–317.
21. Colic, M., Rudolf, R., Anzel, I., Tomic, S. and Lojen, G., The Response of Peritoneal Macrophages to Cu-Al-Ni Shape Memory Alloy, *J. Biomater. Appl*, published online December 11, 2009: doi: 10.1177/0885328209354613.
22. International Standards Organisation. (1977). *Dentistry – Preclinical Evaluation of Biocompatibility of Medical Devices used in Dentistry – Test Methods for Dental Materials, ISO 7404-1*, **1st edn**, Geneva, ISO.
23. Vukovic, G., Marinkovic, A., Obradovic, M. et al. Synthesis, Characterization and Cytotoxicity of Surface Amino-functionalized Water-dispersible Multi-walled Carbon Nanotubes, *Appl. Surf. Sci.*, 2009: **255**: 8067–8075.
24. Soenen, S.J.H., Illyes, E., Vercauteren, D. et al. The Role of Nanoparticle Concentration-dependent Induction of Cellular Stress in the Internalisation of Non-Toxic Cationic Magnetoliposomes, *Biomaterials*, 2009: **30**: 6083–6813.

25. Prnodet, N., Fang, X., Sun, Y. et al. Adverse Effects of Citrate/Gold Nanoparticles on Human Dermal Fibroblasts, *Small*, 2006:**2**: 766–773.
26. Hainfeld, J.F., Slatkin, D.N. and Smilowitz, H.M. The Use of Gold Nanoparticles to Enhance Radiotherapy in Mice, *Phys. Med. Biol.*, 2004: **49**: N309–N315.
27. Vlak, T. and Jajic, I. The Effect of 6 Months of Treatment with Tauredon on Clinical Indicators in Rheumatoid Arthritis, *Reumatizam*, 1992: **39**: 27–31.
28. Kean, W.F., Hart, L. and Buchanan, W.W. Auranofin, *Br. J. Rheumatol.*, 1997: **36**: 560–572.
29. Thorek, D.L. and Tsourkas, A. Size, Charge and Concentration Dependent Uptake of Iron Oxide Particles by Non-Phagocytic Cells, *Biomaterials*, 2008: **29**: 3583–3590.
30. Jiang, W., Kim, B.Y., Rutka, J.T. and Chan, W.C. Nanoparticle-mediated Cellular Response is Size-dependent, *Nat. Nanotechnol.*, 2008: **3**: 145–150.
31. Gesellschaft Deutscher Chemiker. (2008). Goldstäbchen Ohne Gift. Available at: http://www.materialsgate.de/mnews/mn-3569.html (accessed May 10, 2010)
32. Tréguer-Delapierre, M., Majimel, J., Mornet, S., Duguet, E. and Ravaine, S. Synthesis of Non-Spherical Gold Nanoparticles, *Gold Bull.*, 2008: **41**: 195–207.
33. Schedle, A., Samorapoompichit, P., Rausch-Fan, X.H. et al. Response of L929 Fibroblasts, Human Gingival Fibroblasts, and Human Tissue Mast Cells to Various Metal Cations, *J. Dent. Res.*, 1995: **74**: 1513–1520.
34. Verma, A. and Stellacci, F. Effect of Surface Properties on Nanoparticle-Cell Interations, *Small*, 2010: **6**: 12–21.
35. Wataha, J.C., Lockwood, P.E., Schedle, A., Noda, M. and Bouillaguet, S. Ag, Cu, Hg and Ni Ions Alter the Metabolism of Human Monocytes during Extended Low-dose Exposures, *J. Oral Rehabil.*, 2002: **29**: 133–139.
36. Wataha, J.C., Lockwood, P.E. and Schedle, A. Effect of Silver, Copper, Mercury, and Nickel Ions on Cellular Proliferation During Extended, Low-dose Exposures, *J. Biomed. Mater. Res.*, 2000: **52**: 360–364.
37. Wataha, J.C., Lockwood, P.E., Bouillaguet, S. and Noda, M. *In vitro* Biological Response to Core and Flowable Dental Restorative Materials, *Dent. Mater.*, 2003: **19**: 25–31.
38. Schmalz, G., Arenholt-Bindslev, D., Hiller, K.A. and Schweikl, H. Epithelium-Fibroblast Co-Culture for Assessing Mucosal Irritancy of Metals used in Dentistry, *Eur. J. Oral Sci.*, 1997: **105**: 86–91.
39. Wataha, J.C. Biocompatibility of Dental Casting Alloys: A Review, *J. Prosthet. Dent.*, 2000: **83**: 223–234.
40. Medema, J.P. and Borst J.T. Cell Signaling: A Decision of Life and Death, *Hum. Immunol.*, 1999: **60**: 403–411.
41. Leist, M., Single, B., Castoldi, A.F., Kuhnle, S. and Nicotera, P. Intracellular Adenosine Triphosphate (ATP) Concentration: A Switch in the Decision Between Apoptosis and Necrosis, *J. Exp. Med.,* 1997: **185**: 1481–1486.